LOW-COMPLEXITY RECEIVER FOR MASSIVE MIMO-GFDM COMMUNICATIONS

Feng-Cheng Tsai, Fang-Biau Ueng and Ding-Ching Lin

Department of Electrical Engineering,
National Chung Hsing University, Taiwan

ABSTRACT

OFDM has two disadvantages. The first is high peak-to-average power ratio (PAPR), and the second is high out-of-band (OOB) radiated power. In the future communication applications, the diversified scenarios such as Internet of Things, inter-machine communication and telemedicine make the fourth-generation mobile communication no longer applicable. The generalized frequency division multiplexing (GFDM) has a pulse-shaping filter, which has less out-of-band radiated power and peak-to-average power ratio and fewer cyclic prefixes (CP) than OFDM. In order to meet high- data-transmission rate, it is an inevitable trend to install massive multi-input multi-output (massive MIMO) antennas. As the number of antennas increases, so does its complexity. This paper employs time reversal (TR) technology to reduce the computational complexity. Although the number of base station (BS) antennas has increased to eliminate interference, there is still residual interference. In order to eliminate the interference one step further, we deploy a zero forcing equalization (ZF equalization) after the time reversal combination.

KEYWORDS

5G, GFDM, MIMO.

1. INTRODUCTION

The fifth generation (5G) of mobile communications is already developed [1][2], and standards have also been formulated at international conferences. In order to be applied to the Internet of Things (IOT) and Wireless Regional Area Network (WRAN), the 5G system uses high-level technology like massive MIMO [3], beamforming [4] and millimeter wave communication, so that 5G has the advantages of big data transmission rate, low time delay, low power consumption and so on. The development of device-to-device proximity service and machine type communication (MTC) [5] makes OFDM face the challenges of future 5G application scenarios. MTC requires very low power consumption, which makes OFDM's orthogonal subcarriers unbearable; tactile Internet requires short-burst data with low time delay, but OFDM adds long overhead in front of each OFDM symbol. The length of the cyclic prefix (CP) exhibits disappointing spectral efficiency in the performance of the spectrum. The more mobile devices that can connect to the Internet, it means that more spectrum is needed, but our spectrum resources are getting less and less. Because OFDM uses rectangular pulse filters for transmission, its sidelobes are large, resulting in OFDM modulation systems that are sensitive to frequency deviations, high OOB radiated power [6] and high PAPR [7] and other shortcomings, so the application in wireless communication technology is severely restricted.

At present, the known literature proposes several multi-carrier technologies as candidates for 5G communication standards, such as filter bank multicarrier (FBMC) [8], universal filtered multicarrier (UFMC) [9]. The sub-carriers of the FBMC system are all individually pulsed filters, and the sub-carriers have a narrower bandwidth, so the transmission filter has a longer impulse response length. Usually, the length of the filter is four times the signal to reduce OOB emission, and good spectrum efficiency is obtained, but the effect of low time delay cannot be achieved. The UFMC system filters their respective sub-carriers through their respective filters to reduce OOB emissions. Because the bandwidth of filter covers many sub-carriers and the impulse response is very short, high spectral efficiency (SE) can be achieved in transmission. UFMC does not use CP, and the symbol time misalignment in a short period of time is more sensitive than OFDM. The technology used in this paper is GFDM [10]. This technology has a flexible multi-carrier modulation scheme and can be adjusted according to the application of different scenarios [11]. GFDM is a multicarrier modulation technology that uses non-rectangular pulse filters. It uses cyclic convolution to realize the DFT filter bank structure in the frequency domain. GFDM uses less CP [12], which improves the spectrum efficiency to a certain extent. Because GFDM uses non-rectangular filters, it can avoid the problems faced by rectangular pulse filters, namely high PAPR and OOB. There is a special feature in the 5G applications, that is massive MIMO system. However, as the number of antennas increases, the anti-interference ability will saturate at a certain deterministic SINR value, so that the interference will no longer decrease. The computational complexity will also increase as the antenna increases, and its performance will be relatively poor. Therefore, in the 5G large-scale multiple-input multiple-output system, due to the increase in the number of antennas and the increase in the modulation order, designing a technology with computational efficiency is a key challenge. Massive MIMO [13][14] system is an extension of the concept of MIMO system. Usually the number of base station antennas is about 100 or more than 100 [15]. Because each channel is independent, the channels of different users will gradually show orthogonality due to the increase in the number of antennas. This method can eliminate multiple user interference (MUI) [16], and then increase the system capacity. Since the OFDM [17] system faces the problems of high OOB and high PAPR, GFDM can change its sub-carrier waveform according to the selection of different filters and rolling factors, to reduce the OOB radiation power and the PAPR [16]. The multipath effect [18] will make the receiving antennas receive the same signal copy generated by multiple paths. When the multipath delay time is too long, it will cause Inter Symbol Interference (ISI) [19]. In this paper, since we use a large-scale MIMO system, the increase in antennas leads to an increase in computational complexity, so we propose a time reversal [20] method to reduce computational complexity. Time Reversal technology is a basic physical phenomenon that uses the inevitable but abundant multipath radio propagation environment to produce space-time resonance effects, the so-called focusing effect [21]. When the bandwidth is larger, the time resolution is better, and therefore, more multipaths can be displayed. Time reversal technology can use a single antenna to achieve a large-scale MIMO-like effect [22]. By using a large number of virtual antennas, a single-antenna time reversal system can achieve excellent focusing effects in the time and space domains, thereby obtaining the promising performance of massive MIMO systems. In addition, since the time reversal system uses the environment as a virtual antenna array and computing resources, its implementation complexity is much lower. Unlike conventional technologies that use multipath propagation environment, if time reversal technology can use a large enough bandwidth, it does not need to deploy complex receivers or a large number of antennas to take full advantage of multipath propagation [23].

2. SYSTEM MODEL

We assume that there are K users on the transmitting end and M base station antennas. The transmitter uses the GFDM system, which can use less cyclic prefix (CP) than that of the OFDM system, and has a lower OOB and PAPR compared with the OFDM system. The data of the k-th

user can be expressed as (1),

$$u_k = [u_k(0), \dots, u_k(P-1)]^T \quad k \in \{1, 2, \dots K\} \qquad (1)$$

Among them, u represents the data stream, and the subscript k represents the k-th user, which contains sampling elements $p \in \{0, 1, \dots, P-1\}$. Assume that there are K users, each user uses a single-antenna transmission system, and then through symbol mapping according to (1), and then GFDM modulation to GFDM symbol s_k, as in (2),

$$s_k = [s_k(0), \dots, s_k(P-1)] \quad k \in \{1, 2, \dots K\} \quad (2)$$

Next, a cyclic prefix (CP) is added, and the length of the cyclic prefix is usually set to be greater than the length of the multipath channel delay to avoid inter-symbol interference (ISI) caused by multipath. Compared with OFDM, the cyclic prefix length used by GFDM is short to achieve the effect of preventing inter-symbol interference. s_k represents the GFDM symbol obtained by the k-th user's transmission signal through the GFDM modulator, which contains sampling elements $p \in \{0, 1, 2, \dots, P-1\}$. u_k will first enter S/P, pass through the pulse, then pass through the subcarrier filter and finally perform frequency domain offset to obtain s_k. X represents sub-carrier, Y represents sub-symbol, g[n] is the subcarrier filter, e^0 represents the (frequency domain) offset. The mathematical formula of the GFDM symbol generated is expressed as follows,

$$s_k[p] = \sum_{x=0}^{X-1} \sum_{y=0}^{Y-1} g_{x,y}[p] u_k[p] \qquad (3)$$

Among them, u_k is the data symbol, x is the sub-carrier index, y is the sub-symbol index, and p is the sampling index. Here the impulse filter $g_{x,y}[p]$ used by the kth user is a prototype filter after a time and frequency shift version, and the filter used in this paper is a raised cosine filter (RC filter). Among them, the mathematical expression of the raised cosine filter is (4),

$$g_{x,y}[p] = g[(p - mX) \bmod P] \cdot e^{-j2\pi \frac{x}{X} p} \qquad (4)$$

After (3), the transmission symbols are collected and can be expressed as a matrix. We will write all $g_{x,y}[p]$ as a matrix after collecting and sorting.

3. THE PROPOSED DETECTOR

In this paper, we consider a large-scale multi-input multi-output system with multiple users. We consider that there are K users and M BS antenna arrays, and each user is with single antenna. The signal received by the m-th antenna is expressed as follows,

$$r_m = \sum_{k=0}^{K-1} s_k * h_{m,k} + v_m \quad (9)$$

where $s_k = [s_k(0), \dots, s_k(P-1)]$ represents the transmitted signal of the k-th user, r_m represents the received signal of the m-th antenna, and v_m represents the complex additive white Gaussian noise (AWGN). The sequence $h_{m,k} = [h_{m,k}(0), \dots, h_{m,k}(L-1)]$ represents the channel impulse response (CIR) from the k-th user to the m-th BS receiving antenna, where we assume that the

channel is a perfect known channel, the multipath channel tap length is L, and the channels from the user to the BS antenna are independent of each other. Then we write the signal received at the m-th BS antenna as a matrix form after the signal passes through the GFDM modulator, which is expressed as follows,

$$
\begin{aligned}
\bar{r}_m^i &= \sum_{k=0}^{K-1} \left(BH_{m,k}^{(i,i-1)} s_k^{i-1} + BH_{m,k}^{(i,i)} s_k^i \right) + B v_m^i \\
&= \sum_{k=0}^{K-1} \left(BH_{m,k}^{(i,i-1)} A u_k^{i-1} + BH_{m,k}^{(i,i)} A u_k^i \right) + B v_m^i \\
&= \sum_{k=0}^{K-1} \left(\bar{H}_{m,k}^{(i,i-1)} u_k^{i-1} + \bar{H}_{m,k}^{(i,i)} u_k^i \right) + \bar{v}_m^i \quad (10)
\end{aligned}
$$

where $H_{m,k}^{(i,i-1)}$ and $H_{m,k}^{(i,i)}$ are $N \times N$ convolution matrices, s_k^{i-1} and s_k^i respectively represent the tail of symbol time $i-1$ and the head of symbol time i. Matrix $\bar{H}_{m,k}^{(i,i-1)} \triangleq BH_{m,k}^{(i,i-1)} A$ and $\bar{H}_{m,k}^{(i,i)} \triangleq BH_{m,k}^{(i,i)} A$ are the inter-symbol interference matrix and the inter-carrier interference matrix, respectively, where $B = A^{-1}$. We assume that W_p is a combination matrix of $M \times K$, and the number of subcarriers is $p = 0, \dots P - 1$. Generally, there are three common traditional linear combination methods, which are maximum ratio combining (MRC) [24][25], zero-forcing (ZF)[26], and minimum mean square error detection (MMSE).

● Maximum Ratio Combination (MRC):

$$W_p = \bar{H}_p D_p^{-1} \quad (11)$$

● Zero Forcing (ZF):

$$W_p = \bar{H}_p \left(\bar{H}_p^H \bar{H}_p \right)^{-1} \quad (12)$$

● Minimum mean square error (MMSE):

$$W_p = \bar{H}_p \left(\bar{H}_p^H \bar{H}_p + \sigma^2 I_K \right)^{-1} \quad (13)$$

Here, in order to find various interference items in the structure of the large-scale antenna, this paper considers $W_p = \frac{1}{M} \bar{H}_P$. Bring the received signal (10) into equation (11), and after the output of the combiner, the vector of the detection signal is obtained as follows,

$$\hat{u}^i(p) = W_p^H \bar{r}^i(p) \quad (14)$$

where $\bar{r}^i(p) = [\bar{r}_0^i(p), \dots, \bar{r}_{M-1}^i(p)]^T$ is the received signal vector of $M \times 1$, $\hat{u}^i(p) = [\hat{u}_0^i(p), \dots, \hat{u}_{K-1}^i(p)]^T$ is the $K \times 1$ detection signal vector. According to (10) and (11), the detection signal $\hat{u}^i(p)$ can be expressed as follows,

$$
\begin{aligned}
\hat{u}^i(p) &= H_{kk,pp}^{(i,i)} u_k^i(p) + \sum_{\substack{q=0 \\ q \neq p}}^{N-1} H_{kk,pq}^{(i,i)} u_k^i(q) + \sum_{q}^{N-1} H_{kk,pq}^{(i,i-1)} u_k^{i-1}(q) \\
&+ \sum_{\substack{j=0 \\ j \neq k}}^{K-1} \sum_{q=0}^{N-1} \left(H_{kj,pq}^{(i,i-1)} u_k^{i-1}(q) + H_{kj,pq}^{(i,i)} u_k^i(q) \right) + \bar{v}_k^i(p) \quad (15)
\end{aligned}
$$

which includes the inter-symbol interference coefficient, inter-carrier interference coefficient, multi-user interference coefficient and expected coefficient. Because we use a large-scale multiple-input multiple-output system, we can calculate the above coefficients in the form of the law of large numbers. In a large-scale multi-input multi-output system, we can calculate the convergence value by the law of large numbers, so here we propose the multi-user coefficient and explain how to use the law of large numbers to calculate the convergence value. According to (15), the multi-user term can be expanded into the following formula:

$$H_{kj,pq}^{(i,i)} = \frac{\bar{h}_k^H(p)}{M} \left[\left[H_{0,j}^{(i,i)} \right]_{pq}, \dots, \left[H_{M-1,j}^{(i,i)} \right]_{pq} \right]^T \quad (16)$$

$$H_{kj,pq}^{(i,i-1)} = \frac{\bar{h}_k^H(p)}{M} \left[\left[H_{0,j}^{(i,i-1)} \right]_{pq}, \dots, \left[H_{M-1,j}^{(i,i-1)} \right]_{pq} \right]^T \quad (17)$$

where $\bar{h}_k(p) = \left[\bar{h}_{0,k}(p), \dots, \bar{h}_{M-1,k}(p) \right]$ is an $M \times 1$ vector, $[\bar{H}_P]_{m,k} \triangleq \bar{h}_{m,k}(p)$. Before that, let's review the definition of probability. Let a=$[a_1, \dots, a_n]^T$ and b=$[b_1, \dots, b_n]^T$ be two random vectors, and have mutually independent and identically distributed elements. We assume that the i-th element of a and b has $\mathbb{E}\{a_i * b_i\} = C_{ab}, \quad i = 1, \dots, n$. Then according to the law of large numbers, when n approaches infinity, the sampling average $\frac{1}{n} a^H b$ will converge to a distribution average C_{ab}, that is to say $\frac{1}{n} a^H b \to C_{ab}$, $as \ n \to \infty$. When M approaches infinity, (16) and (17) use the form of the law of large numbers into (18) and (19),

$$H_{kj,pq}^{(i,i)} \to \mathbb{E}\left\{ \bar{h}_{m,k}^*(p) \left[\bar{H}_{m,j}^{(i,i)} \right]_{pq} \right\} \quad (18)$$

$$H_{kj,pq}^{(i,i-1)} \to \mathbb{E}\left\{ \bar{h}_{m,k}^*(p) \left[\bar{H}_{m,j}^{(i,i-1)} \right]_{pq} \right\} \quad (19)$$

Since k $\neq$ j, $\bar{h}_{m,k}(p)$ will be the same as $\left[\bar{H}_{m,j}^{(i,i)} \right]_{pq}$ and $\left[\bar{H}_{m,j}^{(i,i-1)} \right]_{pq}$ presents an irrelevant state, so when M approaches infinity, the multi-user coefficients $H_{kj,pq}^{(i,i)}$ and $H_{kj,pq}^{(i,i-1)}$ will approach zero. The coefficients of other terms can be proved as follows after derivation,

$$\left[\bar{H}_{m,k}^{(i,i-1)} \right]_{qp} = \frac{1}{N} \sum_{n=0}^{N-1} \sum_{l=0}^{L-1} h_{m,k}(l) e^{j\frac{2\pi}{N}(nq-lq-np)} \varpi(n-l+N) \quad (20)$$

$$\left[\bar{H}_{m,k}^{(i,i)} \right]_{qp} = \frac{1}{N} \sum_{n=0}^{N-1} \sum_{l=0}^{L-1} h_{m,k}(l) e^{j\frac{2\pi}{N}(nq-lq-np)} \varpi(n-l) \quad (21)$$

$\varpi(n)$ is the window function, and the square function is considered here, which is expressed as follows,

$$\varpi(n) = \begin{cases} 1, & 0 \leq n \leq N-1 \\ 0, & \text{other} \end{cases} \quad (22)$$

When p $\neq$ q, we can get the following calculation process:

$$H_{kk,pp}^{(i,i)} \to \mathrm{E}\left\{ \bar{h}_{m,k}^* \left[\bar{H}_{m,k}^{(i,i)} \right]_{pp} \right\} = \frac{1}{N} \sum_{l=0}^{L-1} (N-l)\rho(l) = 1 - \frac{\tau}{N} \quad (23)$$

$$H_{kk,qp}^{(i,i)} \to E\left\{\bar{h}_{m,k}^* \left[\bar{H}_{m,k}^{(i,i)}\right]_{qp}\right\}$$

$$= \frac{1}{N} E\left\{\sum_n^{N-1} \sum_{l=0}^{L-1} \sum_{l'}^{L-1} h_{m,k}^*(l) h_{m,k}^*(l') \times e^{j\frac{2\pi}{N}(qn-lp+l'p-pn)} \varpi(n-l)\right\}$$

$$= \frac{1-\bar{\rho}(q-p)}{N(1-e^{j\frac{2\pi(q-p)}{N}})} \tag{24}$$

The normalized channel power delay profile is considered in this paper, that is, $\sum_{l=0}^{L-1} \rho(l) = 1$. $\bar{\rho}(q) \triangleq \sum_{l=0}^{L-1} \rho(l) e^{-j\frac{2\pi lq}{N}}$, $\tau \triangleq \sum_{l=0}^{L-1} \rho(l) l$. The method of deriving the values of other ISI coefficients is the same as the above derivation method, where their values are $H_{kj,pq}^{(i,i-1)} \to \frac{\bar{\rho}(q-p)-1}{N(1-e^{j\frac{2\pi(q-p)}{N}})}$ and $H_{kj,pp}^{(i,i-1)} \to \frac{\tau}{N}$.

Continuing the above concept, we can get the following equation by putting the received signal into the time-reversed channel impulse response,

$$r_k^{TR} = \frac{1}{\sqrt{M}} \sum_{m=0}^{M-1} r_m * \beta_{m,k} \tag{25}$$

Among them, r_k^{TR} represents the received signal of the impulse response of k-th users through the time reversal channel, $\beta_{m,k} = \left[h_{m,k}^*(-L+1), \ldots, h_{m,k}^*(0)\right]$ means that on the k-th user, the channel impulse response between the received signal and the corresponding base station antenna is time-reversed to take the conjugate form. Expand the above formula to obtain the following formula,

$$r_k^{TR} = \sum_{j=0}^{K-1} s_j * c_{kj} + v_k^{TR} \tag{26}$$

where s_j represents the j-th GFDM transmission signal, v_k^{TR} represents the k-th AWGN, and c_{kj} is the equivalent impulse response of the original channel and the corresponding time reversal conjugate channel,

$$c_{kj} \triangleq \frac{1}{\sqrt{M}} \sum_{m=0}^{M-1} h_{m,j} * \beta_{m,k} \tag{27}$$

$$v_k^{TR} \triangleq \frac{1}{\sqrt{M}} \sum_{m=0}^{M-1} h_{m,k}^* * v_m \tag{28}$$

when $k \neq j$, c_{kj} presents the crosstalk channel impulse response between terminal k and terminal j; when $k = j$, $c_{kj} = c_{kk}$ is the time reversal equivalent impulse response of the corresponding channel for user k.

Let $r_k^{i\,TR} = \left[r_k^{i\,TR}(iP), \ldots, r_k^{i\,TR}(iP + P - 1)\right]^T$ be a $P \times 1$ vector, $r_k^{i\,TR}$ contains the time-reversal received signal of the i-th time portion, and then expressed in matrix form, the following formula can be obtained,

$$r_k^{i^{TR}} = \sum_{j=0}^{K-1} \left(C_{kj}^{(i,i-1)} s_j^{i-1} + C_{kj}^{(i,i)} s_j^i + C_{kj}^{(i,i+1)} s_j^{i+1} \right) + v_k^{i^{TR}} \quad (29)$$

where $C_{kj}^{(i,i-1)}$, $C_{kj}^{(i,i)}$ and $C_{kj}^{(i,i+1)}$ are the $P \times P$ convolution matrices, which can be expressed as follows,

$$C_{kj}^{(i,i-1)} = \mathcal{T}_{P \times P} \left(\left[c_{kj}(1), \ldots, c_{kj}(L-1), 0_{1 \times 2P-L} \right]^T \right) \quad (30)$$

$$C_{kj}^{(i,i)} = \mathcal{T}_{P \times P} \left(\left[0_{1 \times P-L}, c_{kj}, 0_{1 \times P-L} \right]^T \right) \quad (31)$$

$$C_{kj}^{(i,i+1)} = \mathcal{T}_{P \times P} \left(\left[0_{1 \times 2P-L}, c_{kj}(1-L), \ldots, c_{kj}(-1) \right]^T \right) \quad (32)$$

Among them, they are formed by the way of the Teplitz matrix, which respectively represent the inter-symbol interference matrix and the inter-carrier interference matrix. $c_{kj} \triangleq \left[c_{kj}(1-L), \ldots c_{kj}(L-1) \right]^T$ contains the sampling elements of the time reversal channel impulse response c_{kj}. According to the previous concept, it can be written in another form:

$$\bar{r}_k^{i^{TR}} = \sum_{j=0}^{K-1} \left(\bar{C}_{kj}^{(i,i-1)} u_j^{i-1} + \bar{C}_{kj}^{(i,i)} u_j^i + \bar{C}_{kj}^{(i,i+1)} u_j^{i+1} \right) + \bar{v}_k^{i^{TR}} \quad (33)$$

4. SIMULATION RESULTS

This section compares the performances of large-scale MIMO GFDM system using the traditional equalizers in the previous paper and the TR-ZF method proposed in this paper. We compare the rate performance of each method. The following are the system parameters used in the simulation of this paper.
.

Table 1. Simulation parameters

Modulation Format	4QAM,16QAM
Users(K)	10, 35
Number of Receive Antennas(M)	100, 200
Subcarrier(X)	128
Sub-symbol(Y)	5
Pulse Shaping Filter (g)	RC filter
Roll-Off Factor (a)	0.1
GFDM Demodulator	ZF
Channel Delay(L)	20, 40
Channel	Rayleigh Fading channel

Figure 1 compares the traditional equalizer, the reference paper ZF-FFT, and the TRZF multi-user GFDM system we proposed. The number of users is 10, the number of base station antennas is 100, the channel delay length is 20, and the cyclic prefix length is 20. It can be seen from the figure that when the CP is sufficient, the error rate of the proposed scheme is better than that of the existing ZF and ZF-FFT. Figure 2 compares the traditional equalizer, the reference paper ZF-FFT, and the TRZF multi-user GFDM system we proposed. The number of users is 10, the

number of base station antennas is 100, the channel delay length is 40, and the cyclic prefix length is 20. From the figure, it is found that when the channel delay length is greater than the cyclic prefix length, the traditional ZF and ZF-FFT have poor performance due to increased interference caused by the multipath effect. Figure 3 compares the traditional equalizer, the reference paper ZF-FFT and the TRZF multi-user GFDM system we proposed. 16-QAM is employed, the number of users is 10, the number of base station antennas is 100, the channel delay length is 20, and the cyclic prefix length is 20. When the CP is sufficient, the error rate performance of the proposed scheme is better than that of the traditional ZF and ZF-FFT.
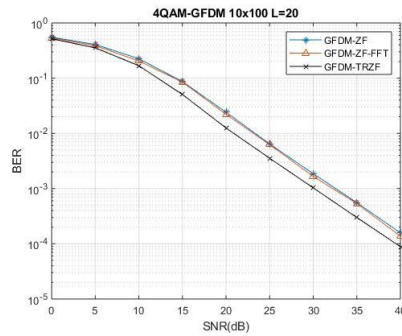
Figure 1.
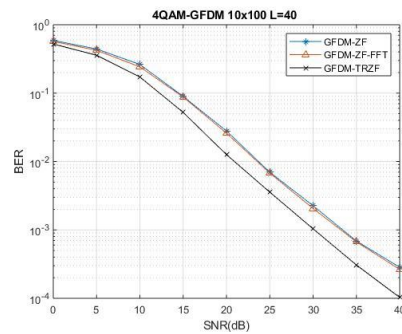
Figure 2.
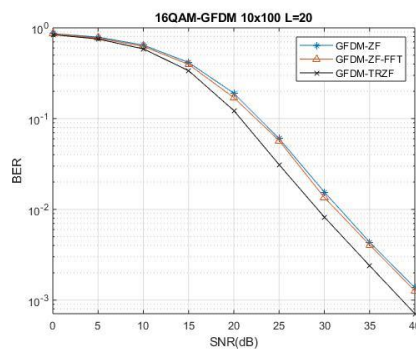
Figure 3.

5. CONCLUSIONS

In a large-scale multiple-input multiple-output system, as the number of antennas increase, channel capacity can be increased and irrelevant noise and interference can be eliminated.

However, an unlimited number of base station antennas will increase computational complexity and SNR can no longer be improved. In this paper, we employ time reversal technology to reduce complexity and improve SNR. When the channel delay length is greater than the cyclic prefix length, compared with the traditional MIMO-GFDM system, the proposed TRZF will not increase the error rate and also reduces the computational complexity.

REFERENCES

[1]   G. Wunder et al., "5GNOW: non-orthogonal, asynchronous waveforms for future mobile applications," in IEEE Communications Magazine, vol. 52, no. 2, pp. 97-105, February 2014.

[2]   G. Fettweis and S. Alamouti, "5G: Personal mobile internet beyond what cellular did to telephony," in IEEE Communications Magazine, vol. 52, no. 2, pp. 140-145, February 2014.

[3]   H. Q. Ngo, E. G. Larsson and T. L. Marzetta, "Energy and spectral efficiency of very large multiuser MIMO systems", *IEEE Trans. Commun.*, vol. 61, no. 4, pp. 1436-1449, Apr. 2013.

[4]   U. Hamid, R. A. Qamar and K. Waqas, "Performance comparison of time-domain and frequency-domain beamforming techniques for sensor array processing," Proceedings of IBCAST, pp. 379-385, 2014.

[5]   Y. Medjahdi et al., "On the Road to 5G: Comparative Study of Physical Layer in MTC Context," in IEEE Access, vol. 5, pp. 26556-26581, 2017.

[6]   J. Van De Beek and F. Berggren, "Out-of-Band Power Suppression in OFDM," in IEEE Communications Letters, vol. 12, no. 9, pp. 609-611, September 2008.

[7]   Y. Xiao, Q. Liang, X. He and S. Li, "On the joint reduction of peak-to-average power ratio and out-of-band power in OFDM systems," in Proc.WCSP, Suzhou, 2010, pp. 1-4.

[8]   A. Jayapalan, P. Savarinathan, P. Mahalingam, A. Dev N.S. and A. Natraj S., "Analysis of Filter Bank Multi carrier Modulation," in Proc. ICCCI, Coimbatore, 2020, pp. 1-4.

[9]   H. Wang and Y. Huang, "Performance evaluation of the universal filtered multi-carrier communications under various multipath fading propagation conditions," in Proc. IEEE iCAST, Taichung, 2017, pp. 466-469.

[10] G. Fettweis, M. Krondorf and S. Bittner, "GFDM- Generalized Frequency Division Multiplexing," in Proc. IEEE VTC Spring, Barcelona, 2009, pp. 1-4.

[11] N. Michailow, I. Gaspar, S. Krone, M. Lentmaier and G. Fettweis, "Generalized frequency division multiplexing: Analysis of an alternative multi-carrier technique for next generation cellular systems," in Proc. ISWCS, 2012.

[12] B. Farhang-Boroujeny and H. Moradi, "Derivation of GFDM based on OFDM principles," in Proc. IEEE ICC, London, 2015, pp. 2680-2685.

[13] A. J. PAULRAJ, D. A. GORE, R. U. NABAR and H. BOLCSKEI, "An overview of MIMO communications - a key to gigabit wireless," in Proceedings of the IEEE, vol. 92, no. 2, pp. 198-218, Feb. 2004.

[14] Wei Hong et al., "Development of the MIMO system for future mobile communications," IEEE/ACES International Conference on Wireless Communications and Applied Computational Electromagnetics, HI, 2005, pp. 634-637.

[15] K. Yamazaki et al., "Field Experimental DL MU-MIMO Evaluations of Low-SHF-Band C-RAN Massive MIMO System with over 100 Antenna Elements for 5G," in Proc. IEEE VTC-Fall, Chicago, IL, USA, 2018, pp. 1-5.

[16] D. A. Feryando, T. Suryani and Endroyono, "Performance analysis of regularized channel inversion precoding in multiuser MIMO-GFDM downlink systems," in Proc. IEEE APWiMob, Bandung, 2017, pp. 101-105.

[17] Y. S. Cho, J. Kim, W. Y. Yang, C. G. Kang, "Introduction to OFDM," in MIMO-OFDM Wireless Communications with MATLAB® , IEEE, 2010, pp.111-151.

[18] M. Cheffena, "Industrial indoor multipath propagation-A physical-statistical approach," in Proc. IEEEPIMRC, Washington, DC, 2014, pp. 68-72.

[19] H. Suganuma, S. Saito, T. Maruko and F. Maehara, "Inter-symbol interference suppression scheme employing periodic signals in coded network MIMO-OFDM systems," in Proc. IEEE Radio and Wireless Symposium (RWS), Phoenix, AZ, 2017, pp. 42-44.

[20] Y. Jin, J. M. F. Moura, N. O'Donoughue and J. Harley, "Single antenna time reversal detection of moving target," 2010 IEEE International Conference on Acoustics, Speech and Signal Processing, Dallas, TX, 2010, pp. 3558-3561.

[21] G. F. Edelmann, H. C. Song, S. Kim, W. S. Hodgkiss, W. A. Kuperman and T. Akal, "Underwater acoustic communications using time reversal", *IEEE J. Ocean. Eng.*, vol. 30, no. 4, pp. 852-864, Oct. 2005.

[22] Y. Han, Y. Chen, B. Wang and K. J. R. Liu, "Time-reversal massive multipath effect: A single-antenna 'massive MIMO' solution", *IEEE Trans. Commun.*, vol. 64, no. 8, pp. 3382-3394, Aug. 2016.

[23] Y. Chen, B. Wang, Y. Han, H. Lai, Z. Safar and K. J. R. Liu, "Why Time Reversal for Future 5G Wireless? [Perspectives]," in IEEE Signal Processing Magazine, vol. 33, no. 2, pp. 17-26, March 2016.

[24] Y. A. Al-Zahrani, N. K. Al-Mutairi, Y. Al-Hodhayf and A. Al-Shahrani, "Performance of antenna selection for maximum ratio combining MIMO system," 2011 IEEE 3rd International Conference on Communication Software and Networks, Xi'an, 2011, pp. 642-645.

[25] H. Lee, J. An, J. Seo and J. Chung, "Multipath Selection Method for Maximum Ratio Combining in Underwater Acoustic Channels," 2018 Tenth International Conference on Ubiquitous and Future Networks (ICUFN), Prague, 2018, pp. 519-521.

[26] H. Wang and R. Song, "Low Complexity ZF Receiver Design for Multi-User GFDMA Uplink Systems," in IEEE Access, vol. 6, pp. 28661-28667, 2018.

[27] W. D. Dias, L. L. Mendes and J. J. P. C. Rodrigues, "Low Complexity GFDM Receiver for Frequency-Selective Channels," in IEEE Communications Letters, vol. 23, no. 7, pp. 1166-1169, July 2019..